

## Global gyrokinetic simulations of $\rho_*$ and $\nu_*$ scalings of turbulent transport

Y. Sarazin 1), G. Dif-Pradalier 1), V. Grandgirard 1), P. Angelino 1), X. Garbet 1), Ph. Ghendrih 1), R. Belaouar 2), N. Crouseilles 2), G. Latu 2), E. Sonnendrücker 2), S. Jolliet 3), B.F. McMillan 3), T.M. Tran 3), L. Villard 3)

1) CEA, IRFM, F-13108 Saint-Paul-lez-Durance, France

2) IRMA-Université de Strasbourg and INRIA Lorraine, France

3) CRPP-EPFL, Association EURATOM-Confédération Suisse, Lausanne, Switzerland

E-mail contact of main author: [yanick.sarazin@cea.fr](mailto:yanick.sarazin@cea.fr)

### Abstract.

Turbulent transport dynamics and level are investigated with the 5D gyrokinetic global code GYSELA, modelling the Ion Temperature Gradient instability with adiabatic electrons. The heat transport exhibits large scale events, propagating radially in both directions at velocities of the order of the diamagnetic velocity. The effective diffusivity is in agreement with that reported in other gyrokinetic codes such as ORB5. Transition from Bohm to gyroBohm scaling is observed on the turbulence correlation length and time, when the normalized gyroradius  $\rho_*$  is decreased from  $10^{-2}$  to  $5.10^{-3}$ . The transition value could depend on the distance to the ITG threshold. Collisions are modelled by a reduced Lorentz-type operator. It allows one to recover theoretical neoclassical predictions in the banana and plateau regimes, namely the heat diffusivity and the mean poloidal flow. In the turbulent regime, preliminary results suggest the turbulent transport increases with collisionality close to the threshold, in agreement with previous publications. Finally, the mean poloidal flow can be increased by about 40% as compared to the neoclassical value.

### 1. Introduction

The confinement properties of magnetized fusion plasmas are governed by the gyrokinetic equation for each species coupled to Maxwell's equations for the electromagnetic fields. The scale invariance of such equations allows one to identify key dimensionless parameters, which are then used to derive empirical scaling law for the energy confinement time normalized to the cyclotron frequency  $\omega_s \tau_E$ . In this framework, the normalized ion gyroradius  $\rho_* = \rho_i/a$  and collisionality  $\nu_*$  are among the most critical. Indeed, IteR will operate at smaller  $\rho_*$  and – to a less extent –  $\nu_*$  values than present day tokamaks, and both exhibit a non vanishing scaling exponent.

Following earlier gyrokinetic publications, we report here the attempt to investigate the scaling properties of turbulence with both  $\rho_*$  and  $\nu_*$  with the 5D GYrokinetic SEmi-LAgrangian code GYSELA. After a brief introduction to the physics accounted for by the code and its numerical performances, the decaying turbulence dynamics is discussed and compared to that obtained with the Particle-In-Cell code ORB5. Evidence of some departure from diffusive-like turbulent transport is reported, reminiscent of the avalanche-like events already reported in flux-driven simulations [1]. The  $\rho_*$  scaling is performed from large to moderate values, still larger than that expected in IteR due to numerical resource limitations. Finally, the last section deals with the role of collisions. The reduced collision

operator implemented in GYSELA is detailed in section 3. First, simulations below the instability threshold are confronted to the predictions of the neoclassical theory. Second, preliminary results in the collisional turbulent regime are reported.

## 2. Turbulence dynamics and $\rho_*$ scaling

GYSELA solves the gyrokinetic equation for the full ion guiding-center distribution  $f(r, \theta, \varphi, v_{\parallel}, \mu)$  in a simple toroidal geometry, where flux surfaces are given concentric circular poloidal cross-sections. All branches of the Ion Temperature Gradient (ITG) turbulence are accounted for, the slab branch and the toroidal one, both for passing and trapped ions. The electrons are adiabatic. Details on the equations can be found in reference [6]. It has been successfully parallelized, achieving very high speed-up performances for the hard scaling test, where the same case is run on an increasing number of processors. Recent upgrades [2] have allowed us to run on 4 096 processors with more than 80% efficiency (93% on 2 048 proc.), fig.1. Domain decomposition together with local cubic spline interpolation [3] have been used in order to achieve such a high efficiency.

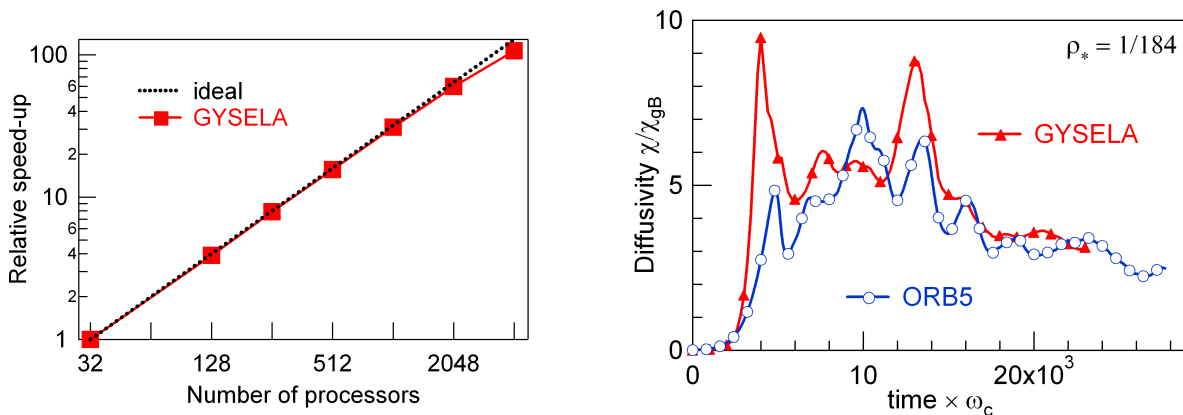


Figure 1: (left) Speed-up achieved with GYSELA for the hard scaling. (right) Time evolution of the turbulent radial diffusivity in ORB5 and GYSELA simulations.

Successful linear and non-linear benchmarks with the CYCLONE test case have already been reported [?, 4, 5]. An additional check is presented on fig.4, showing the system well fulfills the radial force balance equation  $E_r = \nabla_r p/en - v_\theta B_\varphi + v_\varphi B_\theta$ . It can be noticed that the turbulent regime usually exhibits rather low values of toroidal rotation in present simulations. GYSELA has also been compared with the Particle-In-Cell code ORB5 in dedicated collisionless simulations [6, 7]. Although the long term impact turbulent transport has been shown to remain negligible [8], both codes use canonical equilibrium distribution functions [9, 10, 11]. In this framework, the actual density and temperature equilibrium radial profiles are not prescribed as such, but result from the integral over velocity space of  $f_{eq}$ . Therefore, much effort has been successfully devoted to match the initial profiles. Starting from the same initial conditions in terms of temperature and density profiles and magnetic equilibrium, these two global codes exhibit similar

levels of turbulent transport (fig.1) and similar correlation times. The radial boundary conditions slightly differ in both codes: while temperature is kept constant in GYSELA at both ends, the inner temperature is allowed to evolve in ORB5. As a result, in each case, the heat flux coming into the system across the boundaries is not fixed in time. Both codes exhibit profile relaxation due to the back reaction of turbulent flux on mean profiles. Beyond the agreement regarding the effective diffusivity, differences in the gradients and fluxes are observed. The associated physics are difficult to pin down in decaying turbulence and are presently scrutinized.

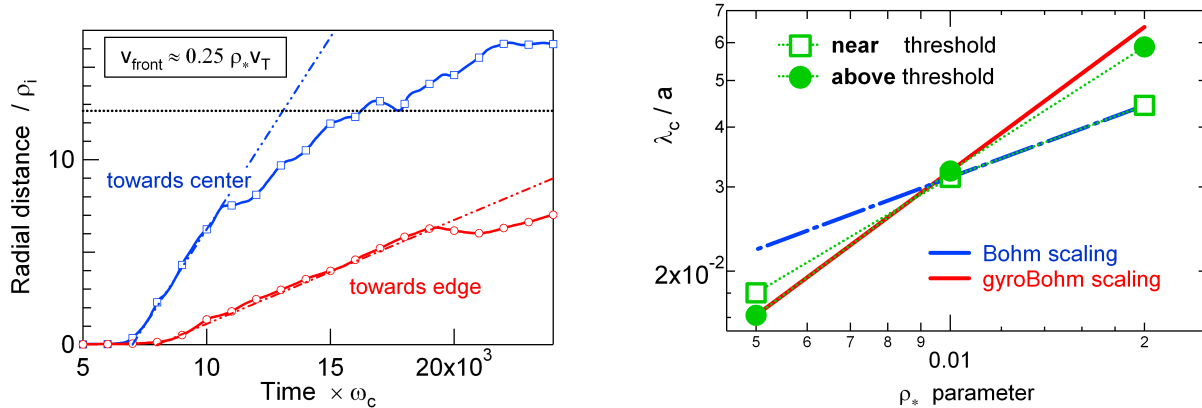


Figure 2: (left) Radial position of the turbulence front when propagating towards the radial boundaries. The horizontal line refers to the buffer zone. (right) Eulerian turbulence correlation length  $\lambda_c$  as function of  $\rho_*$ .  $\lambda_c$  is computed for various values of  $R/L_T$ , either close to or far from the instability threshold. Straight lines refer to Bohm  $\lambda_c/a \sim \rho_*$  and gyroBohm scalings  $\lambda_c/a \sim \rho_*^{1/2}$ .

Although turbulent transport level can be recast in terms of diffusivity, it should be emphasized that the turbulence dynamics features large scale transport events, where steep temperature gradients associated to large heat outflows are propagating on large radial distances (several correlation lengths  $\lambda_c$ ) at fractions of the diamagnetic velocity  $v_* \approx \rho_* v_T$ , with  $v_T$  the thermal speed. Fronts propagating in both directions are observed. Especially such a dynamics leads to the spreading of turbulence towards the buffer regions at radial boundaries, as exemplified on fig.2. The apparent difference in propagation velocity is due to different temperatures, the inner boundary being the hotter. How far the turbulent transport departs from the diffusive description depends on the quantitative role played by such avalanche-like processes.

Regarding the  $\rho_*$  scaling, empirical scaling laws predict a strong dependence (close to gyroBohm) of the energy confinement time on  $\rho_*$ , namely  $\omega_c \tau_E \sim \rho_*^{-2.7}$ , the  $\rho_*$  value expected in Iter is two to three times smaller than in present day tokamaks. This is the major extrapolation parameter in the prediction of the Iter confinement time. In this framework, gyrokinetic simulations have predicted the transition from Bohm to gyroBohm scaling when decreasing  $\rho_*$  [12, 13], the open issues remaining the precise value

of this transition and the underlying physics. Such a scan in  $\rho_*$  has been performed with GYSELA [6] for decaying turbulence. While the correlation time is observed to be roughly independent of  $\rho_*$ , scaling like  $\tau_c \sim c_s/a$ , the correlation length  $\lambda_c$  appears to be consistent with the gyroBohm scaling, namely  $\lambda_c \sim \rho_i$ , at small  $\rho_*$  and well above the linear threshold, fig.2. Conversely, at large values of  $\rho_*$  and close to the threshold, the correlation length exhibits a dependence on the system size  $\lambda_c \sim (a\rho_i)^{1/2}$ , consistently with the Bohm scaling, fig.2. When examining the latter regime, one finds that the gyroBohm scaling appears to be more relevant in the low  $\rho_*$  range thus suggesting that transition value between Bohm and gyroBohm scaling stands between  $\rho_* = 10^{-2}$  and  $\rho_* = 2 \cdot 10^{-2}$  and might depend on the distance to the threshold.

### 3. Neoclassical equilibrium and collisional turbulence

Another key dimensionless parameter could be the plasma collisionality  $\nu_* \sim \nu_{coll}/(v_T/qR)$ . Although it seems well established that  $\omega_c \tau_E$  decreases with  $\nu_*$ , there is no definite empirical scaling, as exemplified on JET [14]. This possibly reflects competing effects. On the one hand, collisions reduce the density of trapped particles, hence lowering the drive for trapped electron and ion modes. On the other hand, collisions damp zonal flows, such that the saturation level of turbulence can increase. This latter mechanism is advocated to explain the increase of turbulent diffusivity with  $\nu_*$ , close to the ITG linear stability threshold [17]. Besides, the poloidal rotation is usually assumed to be governed by neoclassical theory. It is of outmost importance for high confinement regime issues, and especially the triggering of transport barriers.

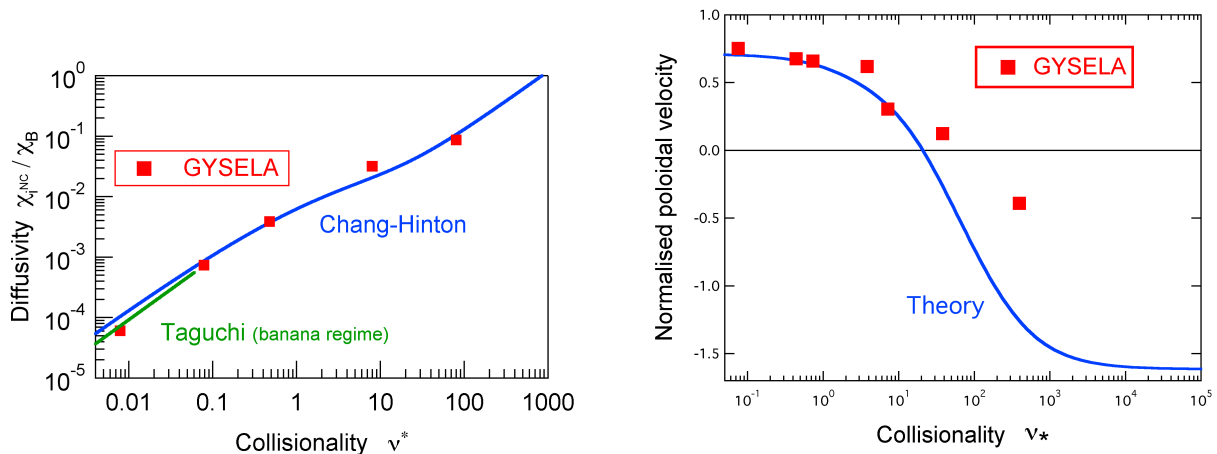


Figure 3: (left) Neoclassical normalised poloidal velocity and (right) neoclassical diffusivity as function of  $\nu_*$ , as computed with GYSELA. The straight lines refer to the neoclassical theoretical predictions.

A Lorentz-type collision operator has been implemented in GYSELA, acting in  $v_{\parallel}$  direction only [8].  $\mu$  remains a motion invariant, hence keeping good parallelization efficiency. It reads  $\mathcal{C}(f) = \partial_{v_{\parallel}} \left\{ \mathcal{D} f_M \partial_{v_{\parallel}} (f/f_M) \right\}$ , with  $f_M = n/(2\pi T/m)^{3/2} \exp(-E/T)$  the

local Maxwellian and  $E = mv_{\parallel}^2/2 + \mu B$ . Here,  $\mathcal{D}$  is a function of  $v = \sqrt{E/T}$ , and proportional to the ion-ion collisionality  $\nu_* = (qR_0/\epsilon^{3/2}v_T)\nu_{ii}$ , with  $\epsilon = r/R$ . Such a reduced operator does not ensure momentum nor energy conservation, since it forces the system to relax towards the centered Maxwellian in  $v_{\parallel}$ , with no parallel mean flow. However, it correctly models the collisional stress tensor. The latter is essential to recover the neoclassical heat transport, while the two former properties would reveal crucial to get the correct particle transport and bootstrap current. Consistently, analytical calculations show that such a simplified operator allows one to recover both the neoclassical heat diffusivity and the poloidal velocity in the banana and plateau regimes [16]. These theoretical predictions are investigated with GYSELA, by running numerical simulations below the linear ITG instability threshold. The results are plotted on fig.3. Good agreement with theory [18] is found for the neoclassical diffusivity over several decades of both  $\chi_{NC}$  and  $\nu_*$ , from the banana to the plateau regime. As far as the neoclassical poloidal rotation is concerned, it is proportional to the ion temperature coefficient  $v_{\theta} = K_1 \nabla_r T_i / eB$ . It is found that the proportionality coefficient  $K_1$  to reverse sign when increasing  $\nu_*$ , as expected theoretically [19]. The plasma rotates in the ion diamagnetic direction at small  $\nu_*$  and in the electron one at larger  $\nu_*$ . Numerical results departs from the theory at large collisionality, possibly indicating the reduced operator becomes irrelevant in the Pfirsch-Schlütter regime.

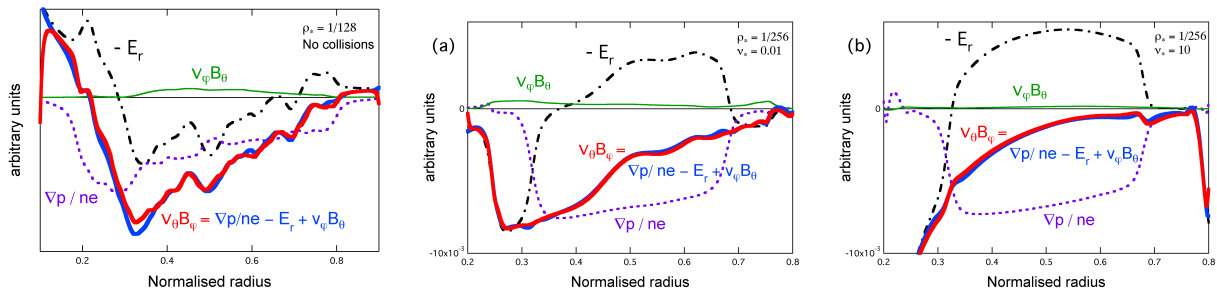


Figure 4: Time averaged profile (in the turbulent regime) of each term entering the force balance equation for  $\nu_* = \{0, 0.1, 10\}$ .

As a result, the weight of the poloidal velocity in the radial force balance depends on  $\nu_*$ . First, in the axisymmetric case, neoclassical theory does not predict the magnitude of the radial electric field  $E_r$ : the prediction deals with the combination  $E_r + v_{\varphi} B_{\theta}$  only. Conversely, whatever  $\nu_*$ , the toroidal rotation is close to zero in the present version of the collision operator, fig.4. This directly results from the lack of Galilean invariance of the operator, which leads to the viscous damping of  $v_{\varphi}$ . Second, the radial electric field is found to almost balance the pressure gradient in the plateau regime, consistently with the fact that  $K_1$  is small in this regime.

While collisions determine the equilibrium poloidal flow, they also efficiently damp zonal flows, as pointed out theoretically [20]. Indeed, they slowly damp the residual flow that survives the linear Landau damping. When pure poloidal flow  $\phi'_{00}(r)$  is initiated in GYSELA, it is observed to decay in time in agreement with theoretical predictions. Such a property is especially important for quantitative predictions on the turbulence

transport level in the collisional regime, since zonal flows are widely believed to govern the turbulence saturation mechanism [21].

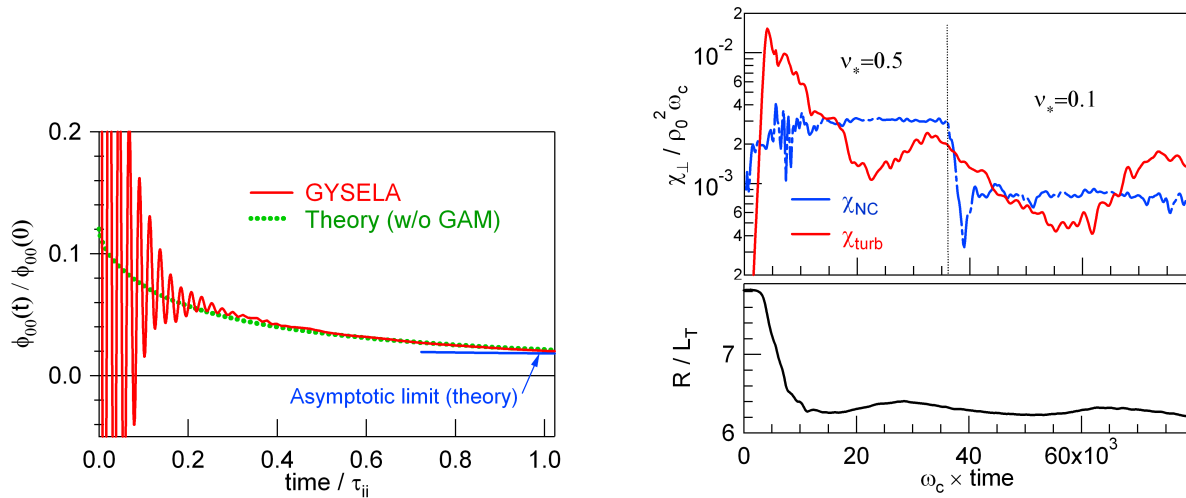


Figure 5: (left) Time relaxation of the poloidal  $E \times B$  flow initiated in GYSELA due to Landau damping and collisions. (right) Time traces of the turbulent and neoclassical heat flux and of  $R/L_T$  when  $\nu_*$  is decreased from 0.5 down to 0.1 at  $\omega_c t = 36.10^3$ .

The impact of collisionality on turbulence and transport is then being investigated by running simulations above the instability threshold. As far as the dependence of the turbulent heat flux on  $\nu_*$  is concerned, it is presently being analyzed for such decaying turbulence simulations in the banana regime, fig.5. When  $\nu_*$  is decreased from 0.5 down to 0.1, the neoclassical transport roughly drops by the same amount. As far as the turbulent flux is concerned, it shows some evidence of reduction, although less pronounced. The large time oscillations make the analysis difficult. The same simulation run at  $\nu_* = 0$  (not shown here) exhibits much weaker turbulent transport, by almost one order of magnitude. Such preliminary results close to the Dimits upshift – where zonal flows are expected to be especially active – look in qualitative agreement with those reported in [17], namely the increase of turbulent transport with collisionality. The detailed understanding of the underlying dynamics remains under investigation.

Two cases are then compared in the banana regime with different  $R/L_T$  – i.e. distances to the threshold, fig.6. It turns out that, at the lowest  $\nu_*$  and close to the threshold, the mean poloidal flow departs from the neoclassical prediction, by about 40%. Conversely, well above the threshold and at larger  $\nu_*$ ,  $v_\theta$  remains almost tied to the neoclassical value. Notice that the turbulent component exhibits similar magnitudes in both cases, of the order of  $10^{-2}v_T$ , while the neoclassical component increases with  $R/L_T$  as discussed earlier.

#### 4. Conclusions:

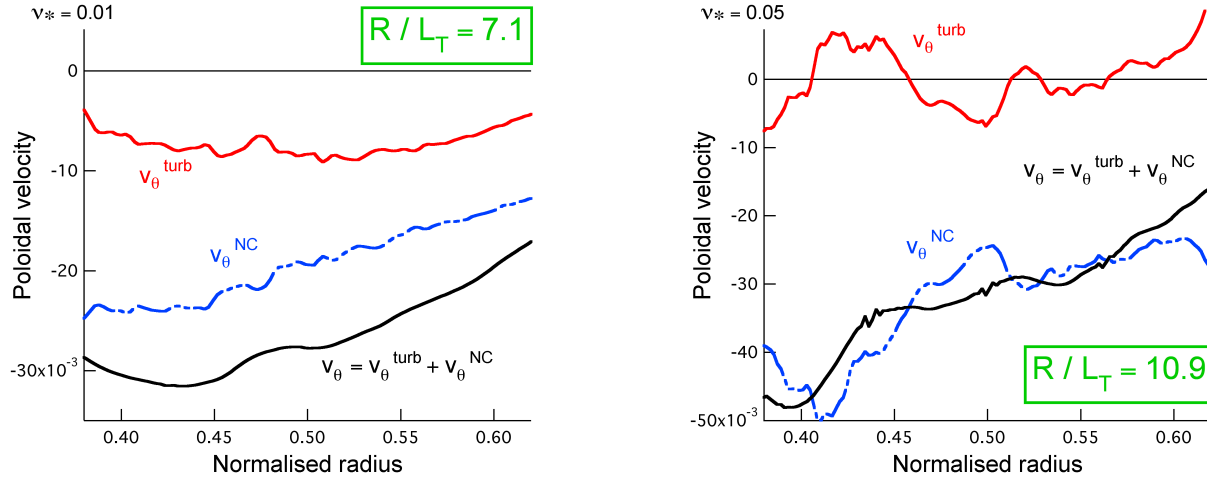


Figure 6: Poloidal velocity profiles in the turbulent regime for  $\nu_* = \{0.01, 0.05\}$  and  $R/L_T$ . The turbulent and neoclassical contributions are also plotted.

Turbulence and transport properties are analyzed with the 5D gyrokinetic GYSELA code, focussing on ITG turbulence in the presence of adiabatic electrons. The turbulent effective heat diffusivity is in the range of other codes such as ORB5. However, the dynamics departs from simple diffusion since it exhibits many avalanche-like transport events. When varying  $\rho_*$  towards ITER values, the turbulence correlation length and time are found to be consistent with gyroBohm scaling. Conversely, it becomes closer to Bohm scaling between  $\rho_* = 10^{-2}$  and  $\rho_* = 2.10^{-2}$ . Such a scaling might also depend on the distance to the threshold. A reduced collision operator acting on  $v_{\parallel}$  only allows one to recover the neoclassical predictions in the banana and plateau regimes. Both the heat diffusivity and the poloidal mean flow agree with the neoclassical theory when simulations are run without turbulence, i.e. below the ITG threshold. In the turbulent regime, preliminary results give credit to the increase of turbulent transport with  $\nu_*$  close to the threshold. Finally, the mean poloidal flow has been observed to depart from the neoclassical one by about 40%.

**Acknowledgements:** This work, supported by the European Communities under the contract of Association between EURATOM and CEA, was carried out within the framework of the European Fusion Development Agreement. The views and opinions expressed herein do not necessarily reflect those of the European Commission.

## References

- [1] B.A. Carreras, D. Newman, V. E. Lynch, and P. H. Diamond, *Phys. Plasmas* **3** (1996) 2903; X. Garbet, Y. Sarazin, P. Beyer et al., *Nucl. Fusion* **39** (1999) 2063
- [2] G. Latu et al., *Recent Advances in Parallel Virtual Machine and Message Passing*, book series Lecture Notes in Computer Science **4757** (2007) (Ed. Springer, Berlin /

- Heidelberg, 2007) 356-364
- [3] N. Crouseilles, G. Latu, E. Sonnendrücker, *Nuclear Instruments Methods in Phys. A* **577** (2007) 129
- [4] V. Grandgirard, Y. Sarazin, X. Garbet et al., *Commun. Nonlinear Science Num. Simul.* **13** (2008) 81–87
- [5] X. Garbet, Y. Sarazin, V. Grandgirard et al., *Nucl. Fusion* **47** (2007) 1206–1212
- [6] V. Grandgirard, Y Sarazin, P Angelino et al., *Plasma Phys. Control. Fusion* **49** (2007) B173
- [7] S. Jolliet et al., *Computer Phys. Commun.* **177** (2007) 409
- [8] G. Dif-Pradalier, V. Grandgirard, Y. Sarazin et al., *Phys. Plasmas*. **15** (2008) 042315
- [9] Idomura Y, Tokuda S, Kishimoto Y, 2003 *Nucl. Fusion* **43** 234
- [10] Angelino P, Bottino A, Hatzky R et al., 2006 *Phys. Plasmas* **13** 052304
- [11] G. Dif-Pradalier, V. Grandgirard, Y. Sarazin et al., *Commun. Nonlinear Science Num. Simul.* **13** (2008) 65–71
- [12] Z. Lin et al., *Phys. Rev. Lett.* **88** (2002) 195004
- [13] J. Candy and R. Waltz, *Phys. Rev. Lett.* **91** (2003) 045001
- [14] D.C. Mc Donald, in *Turbulent transport in fusion magnetised plasmas*, Elsevier Masson SAS, C.R. Physique (ed. X. Garbet) vol. **6** (2006), 584–591.
- [15] G. Dif-Pradalier, V. Grandgirard, Y. Sarazin et al., *Proceedings of the 23rd International School of Plasma Physics on the Theory of Fusion Plasmas*, Varenna Società Italiana di Fisica, Bologna (2008); to be submitted to *Phys. Plasmas*.
- [16] X. Garbet, G. Dif-Pradalier, C. Nguyen et al., *Proceedings of the 23rd International School of Plasma Physics on the Theory of Fusion Plasmas*, Varenna Società Italiana di Fisica, Bologna (2008); to be submitted to *Phys. Plasmas*.
- [17] Z. Lin, T.S. Hahm, W. W. Lee et al., *Phys. Rev. Lett.* **83** (1999) 3645
- [18] C.S. Chang and F.L. Hinton, *Phys. Fluids* **29** (1986) 3314
- [19] Y.B. Kim, P.H. Diamond, R.J. Groebner, *Phys. Fluids B* **3** (1991) 2050
- [20] M.N. Rosenbluth and F.L. Hinton, *Phys. Rev. Lett.* **80** (1998) 724; F.L. Hinton and M.N. Rosenbluth, *Plasma Phys. Control. Fusion* **41** (1999) A653
- [21] P.H. Diamond, S-I. Itoh, K. Itoh and T.S. Hahm, *Plasma Phys. Control. Fusion* **47** (2005) R35–R161